as possible. There are, however, two saliencies built-in which can be exploited to determine the rotor speed. One is caused by the slotting of the rotor and is influenced by the design of the rotor lamination. The second relates to the anisotropy of the lamination material [4]. Though these saliencies are very small and not noticeable in the normal fundamental wave operation of the drive, they can be made visible with the mentioned transient excitation of the machine.

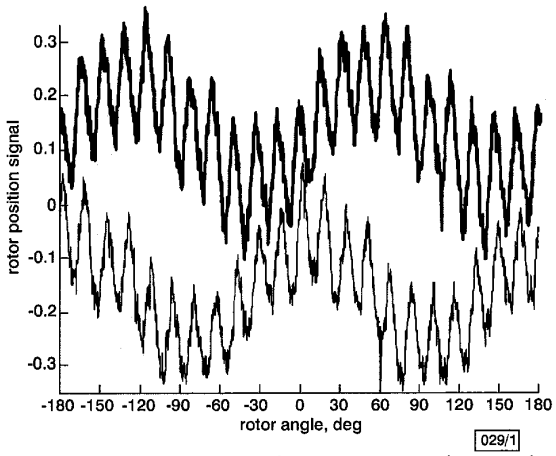

Fig. 1 *Real and imaginary parts of rotor position signal measured with transient excitation on demagnetised standard induction machine*

Offset added for clarity
Lower trace: real part of signal
Upper trace: imaginary part of signal

The measured modulation of the transient reactances of a demagnetised standard induction machine is shown in Fig. 1. The machine was excited with short voltage test pulses impressed by an IGBT inverter. These test pulses consisted of a sequence of positive and negative inverter switching states in the three phases. The two signals in the Figure represent the real and imaginary part of the modulated current change space phasor. The horizontal axis gives the position of the rotor in degrees. On the vertical axis the magnitude of the signals scaled in the internal representation of the signal processor are depicted. During the measurements the rotor was turned one electrical period. The offset of the signals, which represents the mean value of the transient reactances of the machine, can be either eliminated by combining the results of voltage pulses in different phases, or simply by subtraction of the offset value if the pulses are generated only in one phase. To graphically separate the two signal parts in this Figure an additional offset was added.

It can be seen that there are two harmonic components present in the signals caused by the two built-in saliencies mentioned earlier. The modulation caused by the rotor slotting has a fundamental wave with N_R/p periods per pole pair, with N_R as the number of rotor slots and p the number of pole pairs. The machine measured had 44 rotor slots and two pole pairs, leading to 22 revolutions if the rotor is turned one electrical period. The second modulation is generated by the magnetically easy direction of the lamination material which is caused by the special orientation of the crystals as a consequence of the cold rolling and annealing. The magnitudes of the two modulations are of the same order. In principle, it is possible to determine the rotor speed for both of them.

In addition, the magnitudes of the two modulations, as well as their harmonic separation, are fixed by the machine design and do not change with speed. Thus, simple filter algorithms such as phase-locked loops can be used to exploit both harmonics. With a standard fixed point signal processor, the speed of a 44 rotor slot machine with one pole pair can be identified up to a mechanical frequency of ~400Hz, which should be sufficient for most applications. For a higher number of rotor slots, in combination with a high possible mechanical frequency, special filters may be necessary to eliminate the rotor slot harmonic.

A more detailed discussion of the position estimation method is not presented here, this being for the sake of brevity.

Acknowledgment: The author is very much indebted to the Austrian 'Fonds zur Förderung der wissenschaftlichen Forschung', which generously supports the work at the Department of Electrical Drives and Machines at the Vienna University of Technology.

21 February 2001
Electronics Letters Online No: 20010300
DOI: 10.1049/el:20010300

Th.M. Wolbank (*Department of Electrical Drives and Machines, Vienna University of Technology, Gusshausstrasse 25/E372, A-1040 Vienna, Austria*)

E-mail: wolbank@tuwien.ac.at

References

1 SCHROEDL, M.: 'Synchronizing an inverter to a rotating induction motor with unknown magnetizing state', *Electr. Eng.*, 1995, **78**, pp. 51–56
2 HOFFMANN, F., KOCH, S., and WEIDAUER, M.: 'Strategies for magnetizing speed-sensorless induction machines', *Eur. Trans. Electr. Power*, 1999, **9**, pp. 27–33
3 SCHROEDL, M.: 'Sensorless control of AC machines at low speed and standstill based on the inform method'. IEEE IAS Annual Mtg., San Diego, USA, 1996, Vol. 1, pp. 270–277
4 WOLBANK, TH.M., HAIDVOGL, B., and WOEHRNSCHIMMEL, R.: 'Modulation of the transient reactances of inverter fed induction motors by rotor fixed saliencies'. IEEE Int. Symp. Industrial Electronics, Puebla, Mexico, 2000, pp. 207–212

High-Q bulk micromachined silicon cavity resonator at Ka-band

M. Stickel, G.V. Eleftheriades and P. Kremer

A novel bulk silicon micromachining technique for fabricating millimetre-wave waveguide components is presented. This technique enables the formation of deep three-dimensional stacked structures of almost constant cross-section as well as post wafer-bonding metallisation that reduces the effects of air gaps and contact resistances. With these innovations it is possible to realise high-Q devices with low-cost fabrication. Simulated and measured results for a 30GHz silicon cavity resonator are presented.

Introduction: There is presently a growing need for low-loss, high-Q passive components for broadband wireless systems operating at millimetre-wave (mm-wave) frequencies. An important requirement for these components is that their fabrication process must be inexpensive, meaning that systems are produced using low-cost materials with a method conducive to batch-processing. In addition, the components should be easily integrated into a compact, environmentally stable package. This Letter introduces a novel bulk silicon micromachining method for fabricating low-loss mm-wave waveguide components, which can potentially meet these demands.

Novel bulk micromachining topology: Bulk micromachining of silicon is a technology that has been well developed by research groups working on sensors and MEMS [1]. In 1993, McGrath, *et al.* presented the first work in which this technology was used to fabricate metallic waveguides [2]. This group successfully fabricated a low-loss section of W-band (110GHz) waveguide out of two etched silicon wafers that were bonded together.

More recently, there has been an increasing effort to develop waveguide resonators using bulk micromachining of silicon. In 1997, Papapolymerou *et al.* presented a topology where only a single partially etched wafer was used for the cavity [3]. For a 10GHz resonator, this group achieved an unloaded Q-factor (Q_u) of 506. Another group at the University of Michigan used two partially etched high-resistivity silicon wafers to form a K-band cavity in a 'split-block' fashion [4]. This larger cavity produced a higher Q_u of ~1150 at 23GHz.

However, for achieving higher Q-factors, deeper cavities are needed. This implies the utilisation of several stacked silicon

wafers to form the cavities. Such stacked cavities can lead to two significant problems (i) air gaps and finite contact resistances between the stacked wafers, which can severely reduce the overall Q-factor (ii) stacked cavities may result in significantly varying vertical cross-sections due to the sloped sidewalls that originate from the etching process; this can lead to overmoded cavities and higher losses. Therefore, it is clear that there are still some significant issues that need to be addressed in order for bulk-micromachining to be a viable method for realising high-Q, mm-wave components:

(i) Deep 'stacked' cavities of a fixed cross-sectional area must be achievable to increase cavity volume.

(ii) Contact resistances/air gaps at the wafer interfaces must be minimised to maintain high-Q values.

(iii) Alignment of the individual etched wafers needs to be simple and extremely precise.

(iv) Components should be easily integrated with any substrate, eliminating the need for expensive high-resistivity silicon.

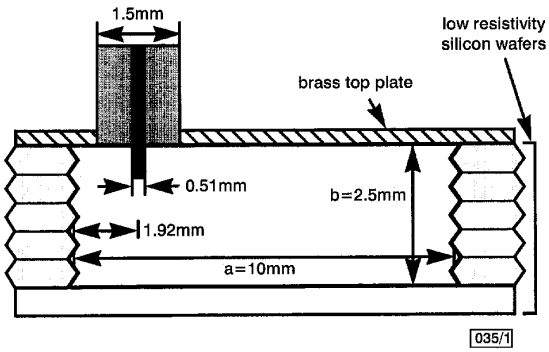

Fig. 1 *Proposed bulk micromachined silicon cavity at 30GHz (length c = 5.8mm)*

To address these difficulties, the micromachined waveguide topology illustrated in Fig. 1 is proposed. This layout utilises double-sided etching, which allows the wafers to be stacked together forming deep cavities of virtually *constant* cross-sectional area. Most importantly, the cavity, excluding the top surface, can be metallised *after* the wafers are bonded together. Therefore, only one critical bond, made between the top plate and the cavity, is required. This post-metallisation reduces the effects of the air gaps that are left after bonding, and results in a higher quality cavity. Also, the individual wafers of the cavity are more easily aligned using this method. Finally, any microwave-quality substrate can be employed to provide the top surface of the cavity. This allows for low-cost, mechanical grade silicon wafers to be used for micromachining, and high-performance mm-wave substrates, such as GaAs, to be used for integration of high-speed electronics.

Ka-band micromachined cavity: A 30GHz cavity has been fabricated using the proposed micromachining topology, and the dimensions are shown in Fig. 1. The cavity was constructed of five sections of 0.5mm thick low-resistivity (doped) silicon wafers. The patterned wafer was simultaneously etched from both sides in a KOH bath. The five identical wafer sections were then visually aligned using gauge blocks as straight edge guides. The five wafers, with the addition of an unetched wafer section for the cavity bottom, were bonded together using a sodium silicate paste. The entire cavity was then metallised using electroless plating of gold for the first seed layers. Electroplating of copper was then utilised to build up the metallisation to an approximate thickness of 25μm. For testing purposes, the cavity was fed with a single coaxial probe placed in a brass plate that formed the top of the cavity.

Return loss measurements of the cavity were made using a Wiltron 360B network analyser, and from these measurements, the unloaded Q-factor was obtained using the procedure outlined in [5]. The simulation and measurement results are summarised in Table 1 and further elaborated below.

Hewlett-Packard's high frequency structure simulator (HFSS) was also used to evaluate the expected, or theoretical Q_u for the fabricated micromachined copper cavity with a brass top. For these simulations, the ideal conductivity of $5.8 \times 10^7 \Omega^{-1}m^{-1}$ was used for the copper metallisation and the brass metallisation was assumed to be $1.57 \times 10^7 \Omega^{-1}m^{-1}$. From Table 1, it can be seen that the Q_u for this cavity is expected to be close to 2600.

Table 1: Simulation and measurement results

	Simulated	Measured		
	Micromachined copper cavity with brass top	Light clamping	Strong clamping	Soldered top
Resonant frequency	29.953GHz	29.982GHz	30.006GHz	29.952GHz
Q_u	2600	960	2050	2155

The first set of measurements were taken with the connection between the top plate and the cavity being made solely through clamping. Return loss results for two degrees of clamping are shown in Fig. 2. The first level of clamping was firm, such that the two pieces were fixed in place and could not be easily moved. The second level was set as tight as possible without damaging the silicon wafers. As is evident from the increase in the size of the resonant loop, the heavy clamping led to an increase in the Q_u from 960 to 2050 (see Table 1).

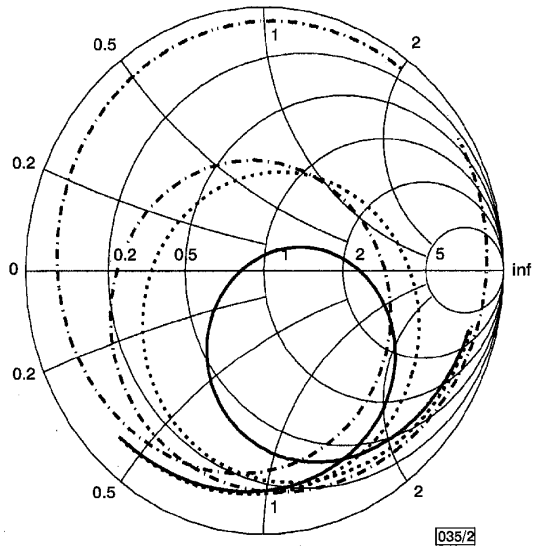

Fig. 2 *Return loss measurements for micromachined cavity*

——— light clamping
····· heavy clamping
— · — soldered connection

Another set of measurements were taken with the same micromachined cavity, this time the top plate was soldered directly to the cavity. This was done by plating a thin layer of tin on the cavity border that interfaces with the top plate. The top plate was fixed in place and the entire structure was heated to complete the soldered connection. This meant that no clamping was required, or used, to increase the Q_u of the cavity. The return loss measurement is also shown in Fig. 2, and the calculated Q_u was 2155. This compares very well with the clamped connection results, and demonstrates that it is possible to achieve stacked high-Q cavities without clamping, thus validating the top-layer bonding process. In addition, this measured Q_u is fairly close to the expected value of 2600. This indicates that the air gaps left between the wafers after bonding were effectively sealed using the post-metallisation technique.

One of the main reasons for the discrepancies between the simulated and measured results is that the uniformity and surface roughness of the cavity metallisation is not comparable to that of a conventional waveguide. This means that the conductivity of copper that was used in the simulations is probably higher than that of the measured cavity. This is due to the difficulty of evenly metallising the cavity with electroplating, since sharp corners remain at its bottom. The authors are presently investigating ways to improve the metallisation process to alleviate this problem.

Conclusions: A new low-cost micromachining technique, which is compatible with standard integrated-circuit fabrication techniques, has been proposed. The advantages of this scheme are that deep stacked cavities of *constant cross-section* are possible, wafers can be easily aligned, integration of high-speed electronics is facilitated, and *post-metallisation* can be used to seal the wafer bonding air gaps. The technique was used to fabricate a 30GHz cavity resonator and excellent results have been achieved. An unloaded Q-factor of 2155 is, to the authors' knowledge, the highest value reported to date for a bulk micromachined cavity at this frequency. Using this technique, other waveguide components, such as filters, couplers and antenna arrays, will be implemented in the future.

22 February 2001
Electronics Letters Online No: 20010313
DOI: 10.1049/el:20010313

M. Stickel, G.V. Eleftheriades and P. Kremer (*Edward S. Rogers Sr. Department of Electrical and Computer Engineering, University of Toronto, 10 King's College Road, Toronto, Ontario, M5S 3G4 Canada*)

E-mail: gelefth@waves.utoronto.ca

References

1 MADOU, M.J.: 'Fundamentals of microfabrication' (CRC Press, New York, 1997)

2 McGRATH, W.R., WALKER, C., YAP, M., and TAI, Y.: 'Silicon micromachined waveguides for millimeter-wave and submillimeter-wave frequencies', *IEEE Microw. Guided Wave Lett.*, 1993, **3**, (3), pp. 61–63

3 PAPAPOLYMEROU, J., CHENG, J., EAST, J., and KATEHI, L.P.B.: 'A micromachined high-Q X-band resonator', *IEEE Microw. Guided Wave Lett.*, 1997, **7**, (6), pp. 168–170

4 BROWN, A.R., BLONDY, P., and REBEIZ, G.M.: 'Microwave and millimeter-wave high-Q micromachined resonators', *Int. J. RF Microw. CAE*, 1999, **9**, (7), pp. 326–337

5 KWOK, R.S., and LIANG, J.: 'Characterization of high-Q resonators for microwave-filter applications', *IEEE Trans. Microw. Theory Tech.*, 1999, **47**, (1), pp. 111–114

SSB MMIC mixer with subharmonic LO and CPW circuits for 38GHz band applications

H.I. Fujishiro, Y. Ogawa, T. Hamada and T. Kimura

A single side-band (SSB) MMIC mixer employing a sub-harmonic configuration with an anti-parallel diode (APD) pair for 38GHz band applications is designed and fabricated. Coplanar waveguide (CPW) models were used to design the mixer circuit. It acts as both an up- and down-converter with a conversion loss of less than 12.4dB and a high image rejection ratio of greater than 15.1dB over a wide frequency range from 32.5 to 42.0GHz.

Introduction: The rapidly increasing demand for higher speeds and wider bands in personal wireless communications has resulted in increased demand for the use of millimetre-wave frequency bands. In millimetre-wave systems, cost effectiveness, low power consumption, mass producibility and superior performance are required. One of the most attractive candidates for millimetre-wave mixer circuits is a sub-harmonic LO configuration using an anti-parallel diode (APD) pair, because it allows the user to reduce the number of LO multiplying stages, acts as both an up- and down-converter with no DC power consumption, and suppresses any even harmonics of LO [1, 2]. A coplanar waveguide (CPW) architecture, in contrast, can be easily mass produced, because it eliminates backside wafer processing and the requirement for via holes [3], and it offers compatibility with flip-chip assembling suitable for low parasitic interconnection [4].

In this Letter, we present a single side-band (SSB) MMIC mixer employing a sub-harmonic configuration with an APD pair and CPW technology for 38GHz band applications. It offers low conversion loss and high image rejection over a wide RF frequency range of 10GHz.

SSB mixer configuration: To achieve a high image rejection ratio in an SSB mixer, precise control of the gain and phase balances over the two signal paths is required [5]. Since the difference in the characteristics of two unit mixers located side by side on an MMIC chip is negligible, imbalances of gain and phase are mainly due to the LO/RF hybrids used.

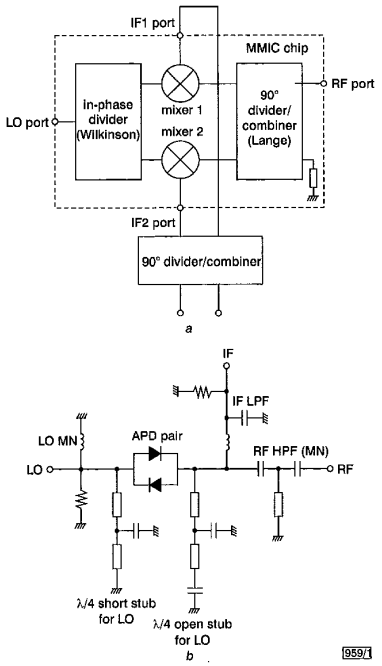

Fig. 1 *Circuit configuration of SSB sub-harmonic mixer MMIC*

a Block diagram
b Circuit diagram of unit sub-harmonic mixer

Fig. 1*a* shows a block diagram of the SSB mixer with subharmonic LO configuration. It consists of two unit sub-harmonically pumped diode mixers, an in-phase divider for the LO signal, and a 90° divider/combiner for the RF signal. A Wilkinson divider is chosen for the LO in-phase divider, which delivers two well-balanced gain and phase signals, because of its symmetric structure. It is constructed using lumped elements without any serious sacrifice in bandwidth, because an LO input frequency, being set to approximately half an RF frequency, is less than the resonance frequency of each element, thus reducing the occupied area. A Lange coupler, chosen for the RF 90° divider/combiner, has very wideband characteristics over an octave. It occupies very little space in the 38GHz band, because the size is proportional to one quarter wavelength of the operating frequency. For the IF signal, an external 90° divider/combiner is used.

MMIC design: Fig. 1*b* shows the circuit diagram of the unit sub-harmonic mixer, which incorporates the APD pair and $\lambda/4$ long short and open stubs for the LO signal [1]. The lengths of both stubs were more than halved using a quasi-lumped technique similar to in [6], in which transmission lines with a characteristic impedance of 71Ω and appropriate shunt MIM capacitors are employed. The $\lambda/4$ long short stub, located towards the LO port, was designed to simultaneously pass the LO signal and block the RF signal. The $\lambda/4$ long open stub, in contrast, located towards the RF port, was designed to block the LO signal and pass the RF signal. An RF highpass filter with a short stub and series MIM capacitors and an IF lowpass filter with a series spiral inductor and a shunt MIM capacitor were also incorporated in the mixer to isolate the RF and LO ports. The RF highpass filter also acted as an RF matching network.

The circuit was designed using CPW technology. As commercial CPW models are not sufficiently accurate or varied, we developed our own CPW models, including transmission lines with several characteristic impedances, discontinuities of bends, tee and cross junctions, lumped elements of spiral inductors and MIM capacitors, hybrids, etc. The Wilkinson divider and the Lange coupler